International Journal of Nanomedicine

Dovepress
open access to scientific and medical research

Open Access Full Text Article

ORIGINAL RESEARCH

Gold Nanoparticles Promote the Bone Regeneration of Periodontal Ligament Stem Cell Sheets Through Activation of Autophagy

This article was published in the following Dove Press journal:
International Journal of Nanomedicine

Yangheng Zhang[1,*]
Peng Wang[2,*]
Yuxian Wang[3,*]
Jiao Li[4]
Dan Qiao[1]
Rixin Chen[1]
Wenrong Yang[5]
Fuhua Yan[1]

[1]Department of Periodontology, Nanjing Stomatological Hospital, Medical School of Nanjing University, Nanjing, Jiangsu, People's Republic of China; [2]State Key Laboratory of Pharmaceutical Biotechnology, Department of Sports Medicine and Adult Reconstructive Surgery, Nanjing Drum Tower Hospital, The Affiliated Hospital of Nanjing University Medical School, Nanjing, Jiangsu, People's Republic of China; [3]College of Biotechnology and Pharmaceutical Engineering, Nanjing Tech University, Nanjing, Jiangsu, People's Republic of China; [4]Department of Orthodontics, Nanjing Stomatological Hospital, Medical School of Nanjing University, Nanjing, Jiangsu, People's Republic of China; [5]School of Life and Environmental Science, Centre for Chemistry and Biotechnology, Deakin University, Geelong, VIC, Australia

*These authors contributed equally to this work

Correspondence: Fuhua Yan
Nanjing Stomatological Hospital, Medical School of Nanjing University, 30 Zhongyang Road, Nanjing, Jiangsu 210008, People's Republic of China
Tel +86 25 8362 0253
Fax +86 25 8362 0202
Email yanfh@nju.edu.cn

Objective: Cell sheet technology (CST) is advantageous for repairing alveolar bone defects in clinical situations, and osteogenic induction before implantation may result in enhanced bone regeneration. Herein, we observed the effect of gold nanoparticles (AuNPs) on osteogenic differentiation of periodontal ligament stem cell (PDLSC) sheets and explored their potential mechanism of action.

Methods: PDLSCs were cultured in cell sheet induction medium to obtain cell sheets. PDLSC sheets were treated with or without AuNPs. Alkaline phosphatase, alizarin red S, von Kossa, and immunofluorescence staining were used to observe the effects of AuNPs on the osteogenic differentiation of PDLSC sheets. Western blotting was performed to evaluate the osteogenic effects and autophagy activity. The cell sheets were transplanted into the dorsa of nude mice, and bone regeneration was analyzed by micro-CT and histological staining.

Results: AuNPs could promote the osteogenic differentiation of PDLSC sheets by upregulating bone-related protein expression and mineralization. The 45-nm AuNPs were more effective than 13-nm AuNPs. Additional analysis demonstrated that their ability to promote differentiation could depend on activation of the autophagy pathway through upregulation of microtubule-associated protein light chain 3 and downregulation of sequestosome 1/p62. Furthermore, AuNPs significantly promoted the bone regeneration of PDLSC sheets in ectopic models.

Conclusion: AuNPs enhance the osteogenesis of PDLSC sheets by activating autophagy, and 45-nm AuNPs were more effective than 13-nm AuNPs. This study may provide an AuNP-based pretreatment strategy for improving the application of CST in bone repair and regeneration.

Keywords: gold nanoparticles, cell sheet technology, bone regeneration, autophagy

Introduction

Alveolar bone defects generally result from periodontitis, trauma, infection, and congenital alveolar fenestration.[1] The clinical effects of traditional treatments, either non-surgical or surgical, are considered to be limited.[2] Regenerative therapy with stem cells has shown promising efficacy in animal models and a few human clinical studies.[3] However, simple implantation of stem cells into bone defects seemed to be insufficient.[4]

To date, many studies have demonstrated that osteogenesis of transplanted cells requires a suitable environment.[4] The usual methods of stem cell therapy involve injection of isolated cell suspensions or the seeding of cells onto scaffolds.[5]

submit your manuscript | www.dovepress.com
DovePress
http://doi.org/10.2147/IJN.S282246

However, the extracellular matrix (ECM) is disrupted when cells are harvested by enzyme digestion.[6] The destruction of adhesive proteins diminishes cell viability and prevents them from integrating with host tissue.[7] Cell sheet technology (CST), in which cells produce their own ECM, provides a new strategy.[5] It could not only greatly improve the utilization and biological activity of stem cells but also provide abundant ECM, which is responsible for transmitting a wealth of biological signals that regulate bone formation.[5]

Periodontal ligament stem cells (PDLSCs) are ideal seed cells for stem cell therapy because of their accessibility, high growth capacity, and multipotency.[4,8] Therapy with PDLSC sheets has shown positive results in alveolar bone defect treatment. In 2010, Feng et al first reported the potential efficacy and safety of autologous PDLSC sheets transplanted onto denuded root surfaces in three patients.[9] Chen et al conducted a randomized controlled trial of 30 periodontitis patients and evaluated the regeneration of autologous PDLSC sheets when combined with bovine-derived bone-mineral materials.[10] Significant height increases and alveolar bone replacement was observed in the test group with no clinical safety issues.[10] Recently, Iwata et al fabricated three-layer PDLSC sheets and found a more substantial increase in alveolar bone height during a six-month follow-up.[11] These results demonstrate the possibility of using PDLSC sheets in clinical applications.

Recently, various attempts have been made to improve the clinical outcomes of CST; these attempts included adding active molecules during culture of the sheets,[12] optimization of scaffold design,[13] and gene transfection.[14] New biocompatible materials, such as nanoparticles, have also been tried.[15] Gold nanoparticles (AuNPs) have been utilized in the fields of drug delivery, diagnostics, and tissue engineering because of their excellent biocompatibility, facile synthetic method, and versatile surface functionalization.[16] Specifically, AuNPs have been developed as promising materials for bone regeneration.[17] It has been reported that AuNPs can promote osteogenic differentiation of mesenchymal stem cells,[18–21] inhibit osteoclast formation,[22] and accelerate bone formation in animal models of bone defects.[23,24]

Our previous studies showed that AuNPs of specific sizes could influence the osteogenic differentiation of PDLSCs.[25] However, whether AuNPs could promote the osteogenic differentiation of PDLSC sheets and improve bone repair in vivo remained unknown. In this study, we aimed to evaluate the osteogenic capacity of PDLSC sheets pretreated with AuNPs in vitro and in vivo, compare the effects of AuNPs of different sizes, and further investigate the possible mechanism involved in this process.

Materials and Methods

Synthesis and Characterization of AuNPs

AuNPs of 13 nm and 45 nm were synthesized and capped with L-cysteine, as described in our previous study.[25] Physical and chemical characterizations of the synthesized AuNPs were carried out by transmission electron microscopy (TEM), dynamic light scattering, and ultraviolet (UV) spectrophotometry.[25]

Isolation and Characterization of PDLSCs

Human PDLSCs were isolated from impacted third molars or premolars extracted for orthodontic treatment by enzyme digestion.[8] To identify putative stem cells, single-cell suspensions (1×10^4 cells) were seeded into 10-cm culture dishes with Dulbecco's modified Eagle's medium (DMEM, Gibco Laboratories, Gaithersburg, MD, USA) supplemented with 1% penicillin/streptomycin (Gibco) and 10% fetal bovine serum (Gibco) and incubated for 10 days at 37°C in 5% CO_2. The colony-forming efficiency was assessed on day 10 with 0.1% toluidine blue. Aggregates of 50 or more cells were scored as colonies. The cell surface markers of PDLSCs were analyzed by flow cytometry.[8] Briefly, approximately 1×10^5 cells were incubated with allophycocyanin (APC)- or fluorescein isothiocyanate (FITC)-conjugated monoclonal antibodies for human CD31, CD45, CD146, STRO-1 (BioLegend, Dedham, MA, USA), CD90, and CD105 (BD Biosciences, San Jose, CA, USA) at 4°C in the dark for one hour. Cell suspensions without antibodies were used as negative controls. After washing, the cells were analyzed using a BD FACSCalibur (BD Biosciences).

Culture and Harvest of PDLSC Sheets

PDLSCs were cultured in six-well plates for 24 hours to allow the cells to reach 80–90% confluence. Then the cell culture medium was replaced by cell sheet induction medium (growth medium supplemented with 50 μg/mL ascorbic acid).[14] After 3 days, the culture medium was replaced with osteogenic induction medium (growth medium supplemented with 0.1 μM dexamethasone, 50 μg/mL ascorbic acid, and 10 mM β-glycerophosphate) containing 10 μM 13- or 45-nm AuNPs. The medium was changed every

3 days. PDLSCs without AuNP treatment served as a control. After 7 or 14 days, cell sheets were evaluated for their osteogenic effects in vitro. After 7 days, cell sheets were harvested from the culture plates with a cell scraper for the in vivo study (Figure 1A).

Structural Observation of PDLSC Sheets

After 7 days of osteogenic induction, PDLSC sheets were harvested, fixed with 4% paraformaldehyde, and embedded in paraffin for hematoxylin–eosin (HE) staining. The thickness of the cell sheets was defined as the average thickness of 10 randomly selected sites in each part of the cell sheet. Then PDLSC sheets were fixed with 2.5% glutaraldehyde, incubated in 1% osmium tetroxide, and embedded in epoxy resin. The ultrastructural changes of the PDLSC sheets were examined using TEM (Hitachi, Tokyo, Japan) at an accelerating voltage of 80 kV.

Alkaline Phosphatase (ALP) Activity Level and Staining

After 7 days of osteogenic induction, PDLSC sheets treated with AuNPs and controls were collected. ALP activity levels were detected using the Alkaline Phosphatase Assay Kit (Abcam, Cambridge, MA, USA) according to the manufacturer's instructions. The absorbance was measured at 405 nm. ALP staining was performed using the BCIP/NBT alkaline phosphatase staining Kit (Beyotime Institute of Biotechnology, Shanghai, China). The staining intensity was observed using an inverted optical microscope (Olympus IMT-2, Olympus Corporation, Tokyo, Japan) and photographed using a digital camera (Canon EOS 70D, Canon Global, Tokyo, Japan).

Mineralized Nodule Staining

After 14 days of osteogenic induction, PDLSC sheets were collected and fixed. For alizarin red S (ARS) staining, cells were incubated with 2% ARS (Sigma–Aldrich, St. Louis, MO, USA) for 5 min, and the staining condition was observed as described above. Then quantitative analysis of ARS staining was performed by incubation for two hours with 10% w/v cetylpyridinium chloride (Sigma–Aldrich) and the absorbance of each well detected at 562 nm. For von Kossa staining, 5% silver nitrate solution (Sigma–Aldrich) was added, and plates were exposed to UV light for one hour. Subsequently, 10% sodium thiosulfate (Sigma–Aldrich) was applied. After incubation for 5 min, the staining condition was observed.

Western Blotting

Proteins were extracted from PDLSC sheets with different treatments. Primary antibodies were purchased from Abcam (anti-Runt-related transcription factor 2 (Runx2), anti-ALP, anti-collagen 1 (COL1), anti-osteopontin (OPN), and anti-sequestosome 1/p62 (p62)) or Cell Signaling Technology (anti-LC3) (Danvers, MA, USA). The blots were imaged using a chemiluminescent imaging system (Tanon Science & Technology Co., Ltd., Shanghai, China).

Immunofluorescence Staining

The bone-related proteins Runx2 and ALP were detected by immunofluorescence. Secondary antibodies conjugated with Alexa Fluor 594 (ThermoFisher Scientific, Waltham, MA, USA) and 4′-6-diamidino-2-phenylindole (DAPI; Sigma–Aldrich) were used for visualization. Immunofluorescent signals were viewed using a confocal laser scanning fluorescent microscope (Nikon Instruments Co., Inc., Tokyo, Japan).

Fabrication of Sheet–Scaffold Constructs

Biphasic tricalcium phosphate (BCP) ceramics (with a hydroxyapatite-to-tricalcium phosphate ratio of 3:7, average void volume of 70%, core diameter of 100–400 μm, diameter of 5 mm, and thickness of 2 mm) were purchased from the National Engineering Research Center for Biomaterials of Sichuan University (Chengdu, China). The BCP ceramics were soaked in culture medium overnight and dried. BCP scaffolds were wrapped in control or AuNP-treated cell sheets (Figure 1B and C). The constructs were then immersed in media for 2 hours to allow cell sheet adhesion to the scaffold surface.

Additionally, PDLSC sheets labeled by green fluorescent protein (GFP) were used to determine whether the transplanted cells would survive in vivo. PDLSC cultures were infected with adenovirus vector harboring enhanced GFP (GenePharma, Shanghai, China). Transfection was carried out according to the manufacturer's instructions. GFP-positive PDLSC sheet–scaffold constructs were fabricated as described above.

Subcutaneous Implantation

Six-week-old immunodeficient male mice were obtained from the Model Animal Research Center of Nanjing University. Two small incisions were made longitudinally along the central line on the dorsal surface of each mouse, and four subcutaneous pockets were made by blunt

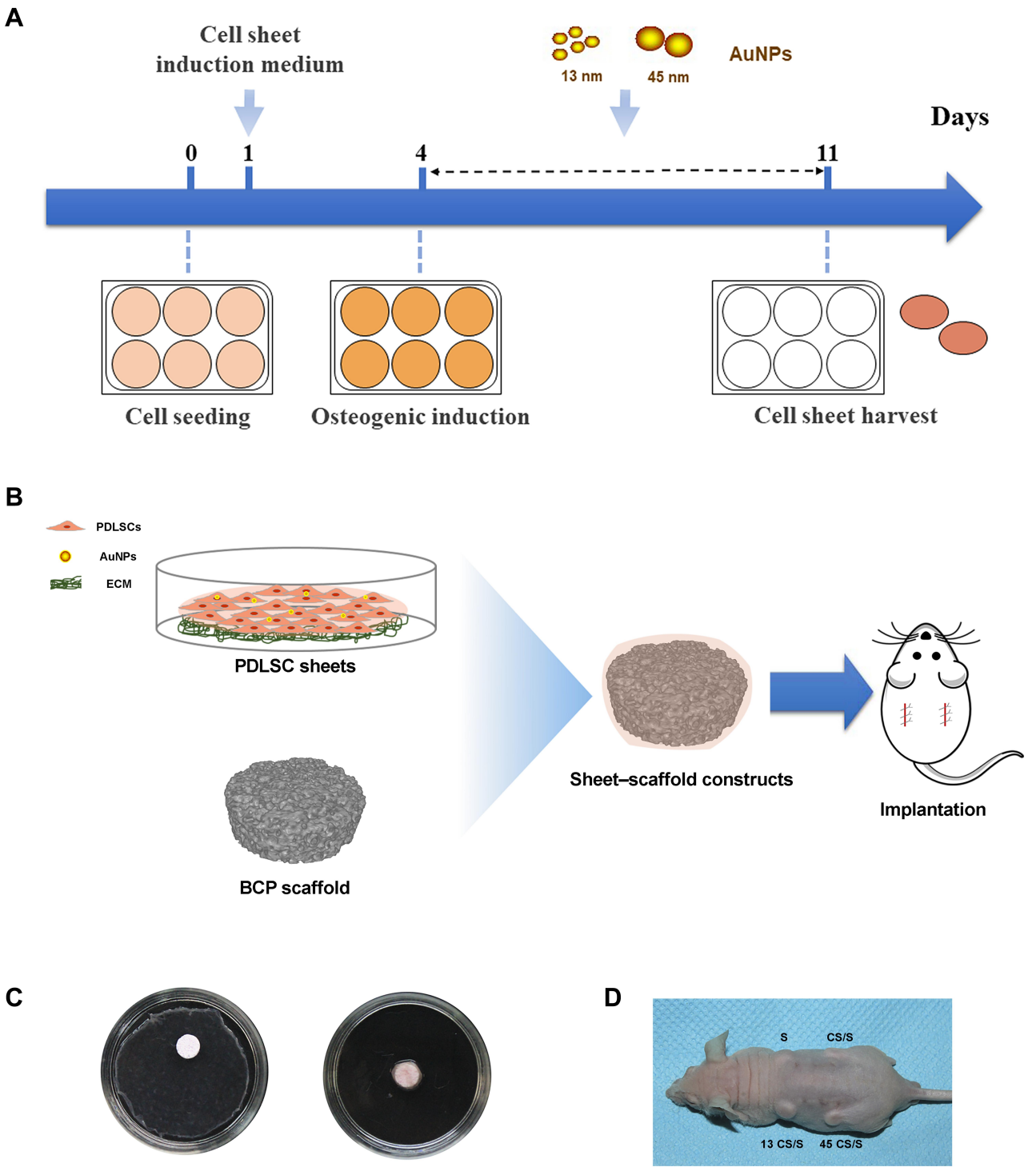

Figure 1 (**A**) Scheme for the in vitro study. (**B**) Scheme for the in vivo study. (**C**) Fabrication of sheet–scaffold constructs. (**D**) The constructs were implanted into the dorsa of nude mice at 1 week.

dissection. The subcutaneous pockets were divided into four groups: BCP scaffold without cell sheet (S); PDLSC sheet/BCP (CS/S); PDLSC sheet treated with 13-nm AuNPs/BCP (13 CS/S); and PDLSC sheet treated with 45-nm AuNPs/BCP (45 CS/S). Each individual pocket held one scaffold, or a scaffold wrapped with cell sheets (pockets selected randomly), and the incisions were closed with surgical sutures. After 8 weeks, the transplants were harvested and fixed with 4% paraformaldehyde for further analysis. For GFP-positive PDLSC sheet–

scaffold constructs, implants were harvested after 4 weeks, and the sections near the central area of the implants were observed with a confocal laser scanning fluorescent microscope to confirm the survival of the transplanted cells.

Micro-CT Analysis

To evaluate bone regeneration, implants were scanned with a SkyScan 1176 scanner (Bruker micro-CT, Kontich, Belgium) using the following parameters: pixel size of 17.76 μm, source voltage of 90 kV, and source current of 278 μA. The images were reconstructed using NRecon software (Bruker). Segmentation and reconstruction of the scaffolds were performed by thresholding with image-processing software (CTAN, Bruker). Three-dimensional representations of the constructs were generated from the micro-CT data using CTVOL (Bruker).

Histology and Immunohistochemical Analysis

Implants were decalcified with 10% ethylenediaminetetraacetic acid (EDTA) for 2 weeks, dehydrated in an ethanol series, and embedded in paraffin. Paraffin sections were analyzed by HE staining and bone-specific staining (Goldner's trichrome, Toluidine blue, and Masson staining; all kits were purchased from Solarbio Life Sciences, Beijing, China). Osteoprotegerin (OPG), OPN, and osteocalcin (OCN) expression were detected by immunohistochemical analysis. Primary antibodies were purchased from Abcam (OPN) or Proteintech (OPG and OCN) (Wuhan, China). The UltraVision Quanto Detection System HRP DAB (ThermoFisher Scientific, CA, USA) was used for visualization. The immunohistochemical staining was scored by measuring the integrated optical density (IOD) of at least six images from each slice.

Statistical Analysis

The quantitative analysis of images was performed using ImageJ. All data were presented as means ± SD. One-way ANOVAs or t-tests were used to evaluate differences using SPSS Statistics 20 software (IBM, Armonk, NY, USA). A two-tailed $p<0.05$ was considered statistically significant.

Results

Characterization of PDLSCs

Single-cell suspensions from human periodontal ligaments were seeded at low density (1×10^4 cells); approximately 20 adherent clonogenic cell clusters formed (Fig. S1A). This colony-forming cell population was named PDLSCs. These cells exhibited typical fibroblastic morphology (Fig. S1B). The results of the flow cytometry analysis of markers related to mesenchymal stem cells are shown in Figure S1C. Almost all the PDLSCs expressed CD90 and CD105 (>99%). CD146 and stromal cell surface marker-1 (STRO-1) were expressed on 59.5% and 9.6% of PDLSCs, respectively. However, CD31 (an endothelial stem cell marker) and CD45 (a hematopoietic stem cell marker) expression was low (<1%).

Characterization of AuNP-Treated and Control PDLSC Sheets

After being cultured in sheet-induction medium (containing ascorbic acid) for 3 days followed by osteogenic induction medium for 7 days, the margins of the cell sheets contracted spontaneously, which suggested they were mature and could be harvested. HE staining results revealed that the harvested PDLSC sheets were two- or three-layered. The thicknesses of the cell sheets treated with AuNPs (13 nm and 45 nm) were slightly thicker than those of the controls (Figure 2B), although there was no significant difference between the three groups.

Effects of AuNPs on Osteogenic Differentiation of PDLSC Sheets in vitro

PDLSC sheets treated with AuNPs expressed ALP to a higher degree than the controls (Figure 2C). However, there was no significant difference between the 13 CS and 45 CS groups. Mineral deposition was visualized by ARS and von Kossa staining. Mineralized nodules were increased in PDLSC sheets treated with AuNPs (Figure 2C), and sheets treated with 45-nm AuNPs showed much stronger mineralized nodule formation compared with sheets treated with 13-nm AuNPs. The mineralization was increased about 2–4 times compared with the control by 45-nm AuNP treatment (Figure 2C). The effects of AuNPs on Runx2, ALP, COL1, and OPN protein expression were determined by Western blotting. As shown in Figure 3A, 13-nm and 45-nm AuNPs upregulated these osteogenic markers, and the stimulative effect of 45-nm AuNPs was better than that of 13-nm AuNPs. The osteogenic marker proteins' levels in the 45 CS group were twice those of the control group. Moreover, cell immunofluorescence showed that Runx2 and ALP were highly expressed in PDLSC sheets treated with AuNPs, and

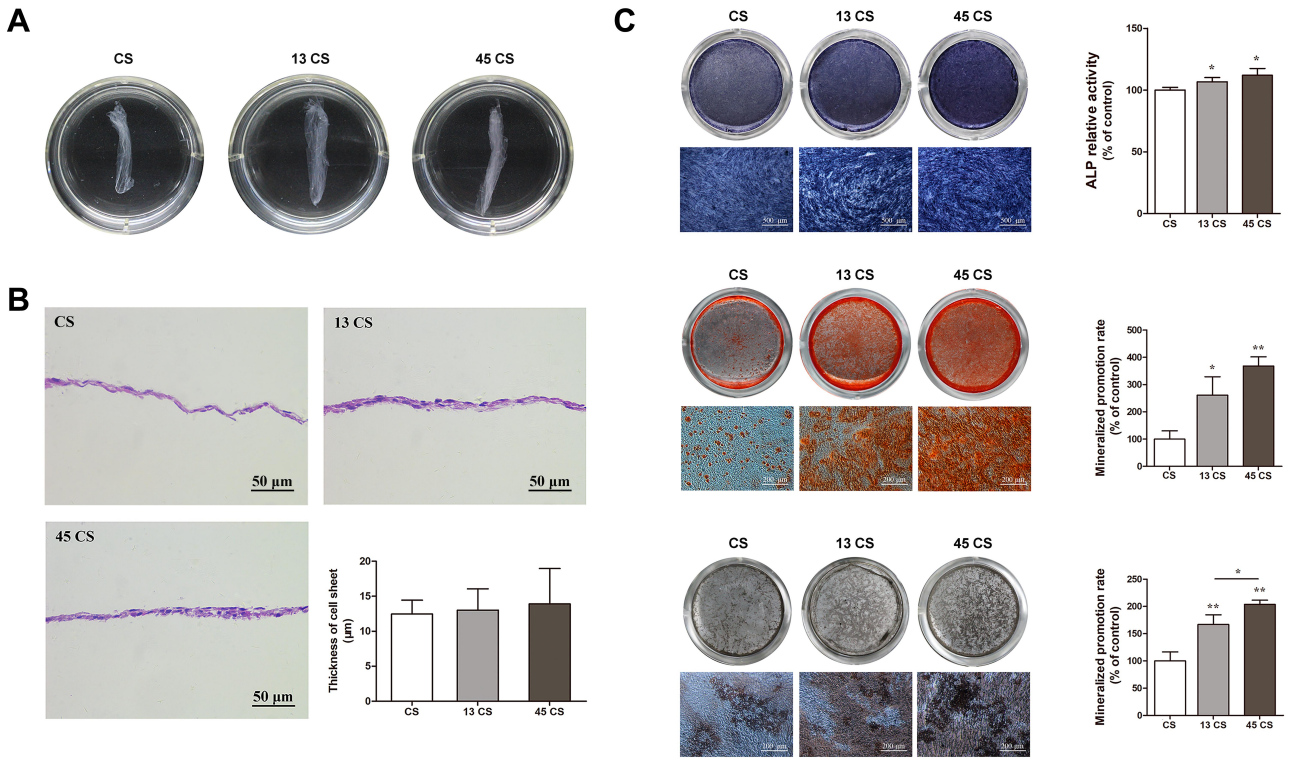

Figure 2 Characterization and osteogenic differentiation of AuNP (13 nm and 45 nm)-treated and control PDLSC sheets. (**A**) PDLSC sheets of different groups. (**B**) Representative images of HE staining and quantification. (**C**) ALP, alizarin red S, and von Kossa staining and quantification. *p<0.05, **p<0.01.

higher expression was observed in the 45 CS group (Figure 3B), which was similar to the Western blot results.

Involvement of Autophagy in the Effect of AuNPs on PDLSC Sheets

To evaluate autophagic changes in PDLSC sheets treated with AuNPs, the expression of the autophagy markers LC3 and p62 was examined. AuNPs of 13 nm and 45 nm both increased LC3-II expression and reduced p62 expression. Specifically, 45-nm AuNPs more effectively upregulated autophagic activity than 13-nm AuNPs (Figure 4A). Furthermore, the TEM images showed that PDLSC sheets treated with AuNPs accumulated double-membrane autophagosomes (Figure 4B).

Fabrication of PDLSC Sheet/BCP Constructs and Tracking of Implanted PDLSCs

To determine whether the transplanted cells survived in vivo, PDLSC sheets were labeled by GFP before transplantation (Fig. S2A). After 4 weeks, green fluorescence could still be observed in the PDLSC sheet/BCP constructs, which confirmed that PDLSCs survived and proliferated inside the scaffold. The expression of green fluorescence was also in agreement with the HE-staining results (Fig. S2B).

In vivo Bone Formation of PDLSC Sheet/BCP Constructs

The micro-CT results indicated 3D construction of new bone formation within BCP scaffolds 8 weeks post-surgery. There was a marked increase in new bone formation in both groups treated with AuNPs. In the S (only BCP scaffolds) and CS/S groups, the regenerated tissues were punctiform and small, whereas those in the 13 CS/S and 45 CS/S groups were clumpier and larger (Figure 5A).

The histology results showed that new bone grew into the pores of the BCP scaffolds (Figure 5B). In groups treated with 13-nm and 45-nm AuNPs, clustered AuNPs could be observed both on the surface of scaffolds and inside the interconnected pores (Fig. S3). Furthermore, histological staining with Goldner's trichrome and toluidine blue confirmed more new osteoid formation in the AuNP-treated groups (Figure 5C). Masson staining showed greater collagen accumulation in AuNP-treated groups (Figure 5C). More bone structures and collagen formation were found within the constructs treated with

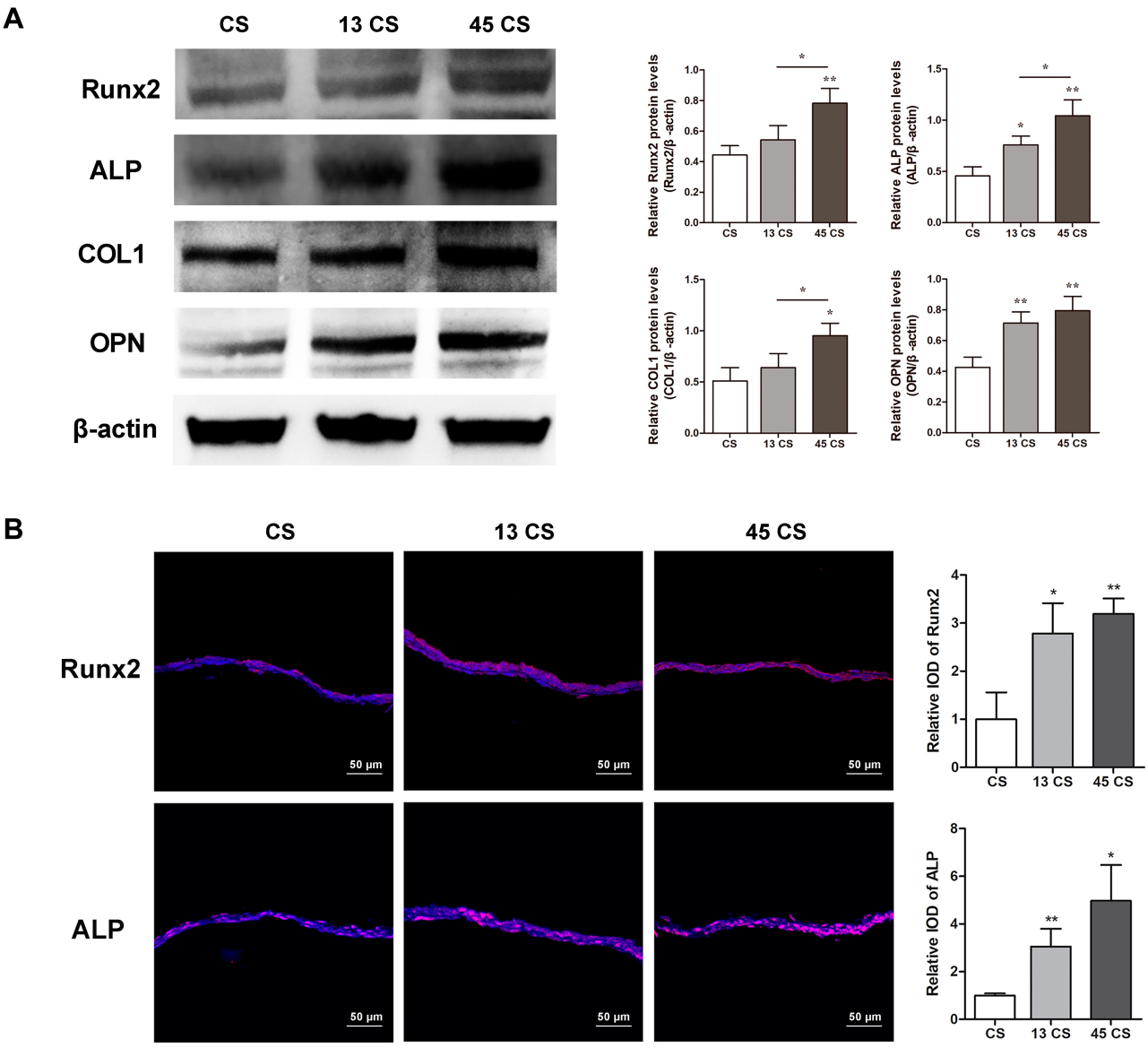

Figure 3 Osteogenic protein expression in PDLSC sheets. (**A**) Western blot of Runx2, ALP, COL1, and OPN and quantification. (**B**) Immunofluorescent analysis of Runx2 and ALP expression and quantification. *p<0.05, **p<0.01.

45-nm AuNPs than those treated with 13-nm AuNPs (Figure 5C).

In vivo Expression of Osteogenic Proteins in PDLSC Sheet/BCP Constructs

Immunohistochemical (IHC) staining for osteogenic markers (OPG, OPN, and OCN) was performed in the newly regenerated tissue. Compared with the S group, more intense positive staining was observed in all cell sheet groups (Figure 6). Quantitative analysis indicated that constructs pretreated with 13-nm AuNPs expressed more OPG than the CS/S group. 45-nm AuNPs showed significantly higher expression of OPG, OPN, and OCN than the CS/S and 13 CS/S groups. These results indicated that 45-nm AuNPs were the most efficient at activating the expression of bone markers Osteogenic protein expression in PDLSC sheet/BCP constructs. (Figure 6).

Discussion

The present study is a brand-new attempt to evaluate the osteogenic effects of AuNPs in a preclinical model based on our previous work.[25] It showed that AuNPs, especially 45-nm AuNPs, could promote the osteogenic differentiation of PDLSC sheets in vitro and in vivo.

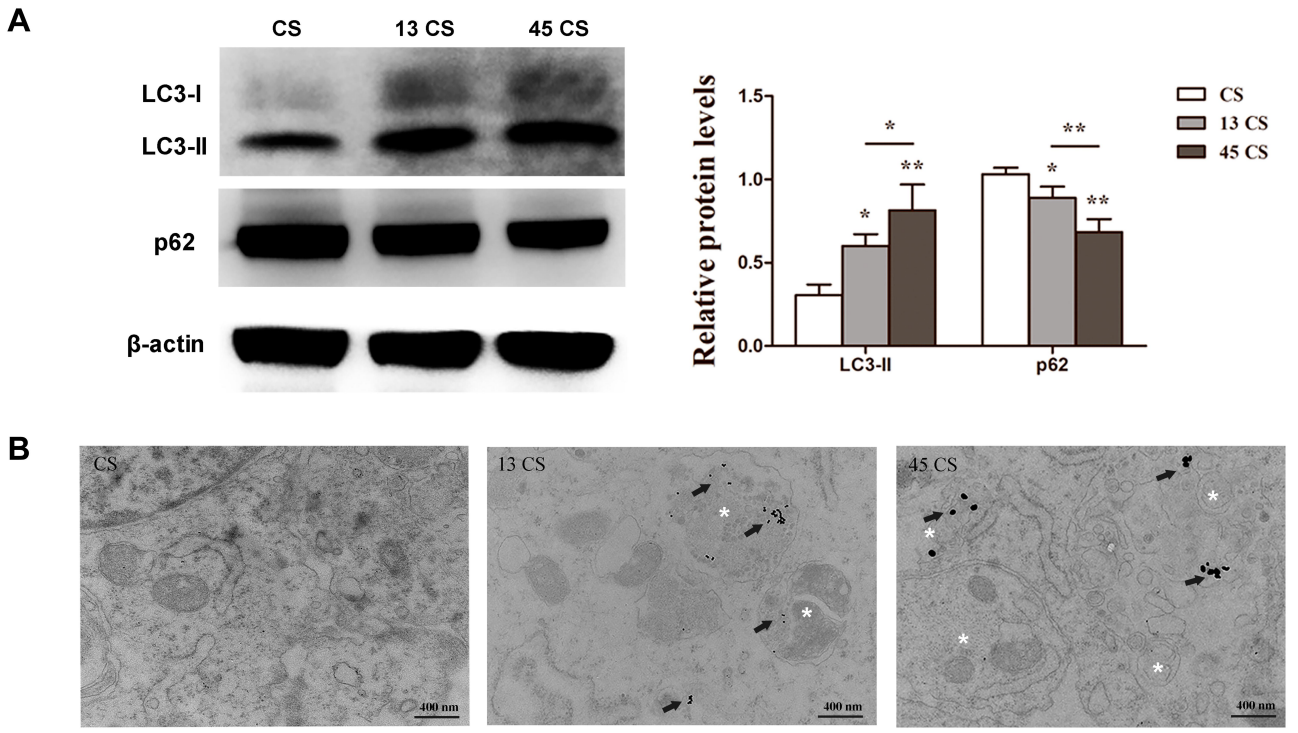

Figure 4 Effects of 13-nm and 45-nm AuNPs on autophagy of PDLSC sheets. (**A**) Western blot of LC3, p62, and quantification. (**B**) TEM images; arrows indicate internalized AuNPs, and the white "*"Indicates autophagosomes. *p<0.05, **p<0.01.

PDLSCs have good prospects in clinical applications because of their availability and effectiveness. In this study, PDLSCs isolated from the root surface were positive for CD90, CD105, CD146, and STRO-1 and negative for CD31 and CD45, which indicated that PDLSCs remained stem cell-like.[8] However, many factors influence cell-based therapies, such as insufficient cell numbers, low cell utilization rate, poor adhesion efficiency, uneven cell distribution, disturbed microenvironment, and difficulty guiding the direction of differentiation.[26]

CST was chosen because of its ability to load a large number of cells and its endogenous ECM.[27] ECM produced by resident cells has a 3D structure that supports cell attachment, migration, and behavior.[28] In addition, ECM contains bioactive cues, such as growth factors, functional peptides, and polysaccharides, which could promote cell proliferation and differentiation.[29] In this study, ascorbic acid was used to increase ECM generation and accelerate the formation of cell sheets.[30] PDLSC sheets with tight junctions between cells and abundant ECM could be detached from culture dishes and harvested for transplantation.

PDLSC sheet transplantation has been used clinically for bone regeneration. A few clinical studies revealed that patients treated with PDLSC sheets exhibited significant bone replacement in the alveolar bone with no adverse reactions.[9–11] How to improve effectiveness by controlling cell differentiation status is another challenge. Recent attempts, mainly by the application of growth factors and biological mediators, have been made to enhance osteogenesis.[12,31,32] It was reported that addition of bone morphogenetic protein-2 or stromal cell-derived factor-1 into cell sheets could induce more bone regeneration.[31,32] However, it is difficult to control the degree of mineralization reaction because of these proteins' strong and immediate effects.

Nanomaterials have been proven to be alternative regulators of cell differentiation.[15] Nanoparticles, including gold, silver, and iron oxide nanoparticles, have been studied as materials for this purpose.[18,33,34] AuNPs have been reported as a new type of osteogenic agent for bone regeneration.[17] In our previous study, it was found that AuNPs could promote osteogenic differentiation of PDLSCs in a size-dependent manner. AuNPs with sizes of 45 nm showed better osteogenic effects than 13-nm AuNPs.[25] However, there has been no study evaluating the effects of AuNPs on cell sheet osteogenesis. This study showed that AuNP supplementation enhanced the

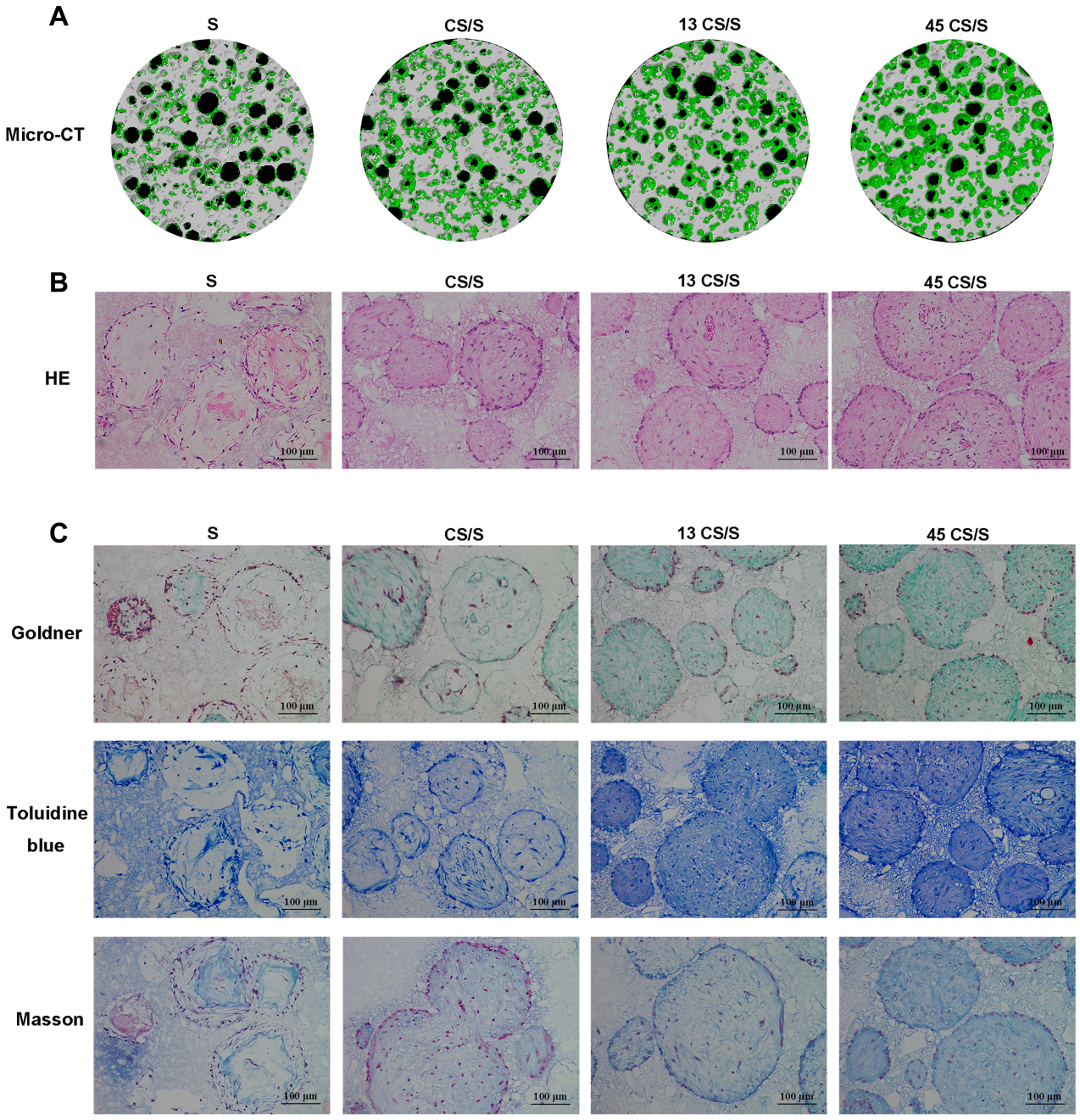

Figure 5 Bone formation of PDLSC sheet/BCP constructs in vivo 8 weeks post-surgery. (**A**) Representative images of micro-CT. (**B**) HE staining. (**C**) Goldner's trichrome, toluidine blue, and Masson staining.

osteogenic differentiation of PDLSC sheets. Moreover, the groups treated with 45-nm AuNPs showed better osteogenic differentiation and ECM mineralization, which was consistent with what we found about the effects of AuNPs on PDLSCs in our previous study.[25]

In this study, PDLSC sheets pretreated with AuNPs were slightly thicker than controls, which indicated that AuNPs could induce greater ECM production (Figure 2A). After osteogenic induction, the AuNP groups had significantly higher levels of ALP activity and mineralized nodule formation compared with controls (Figure 2C). Expression levels of the bone-related marker proteins Runx2, ALP, COL1, and OPN reacted similarly (Figure 3A and B). In fact, Runx2 transcription occurs during the initial stage of osteogenic differentiation and triggers expression of other bone-related genes.[35] ALP is an osteoblastic metabolic enzyme involved in mineral deposition.[36] These two early indicators initiate the process of

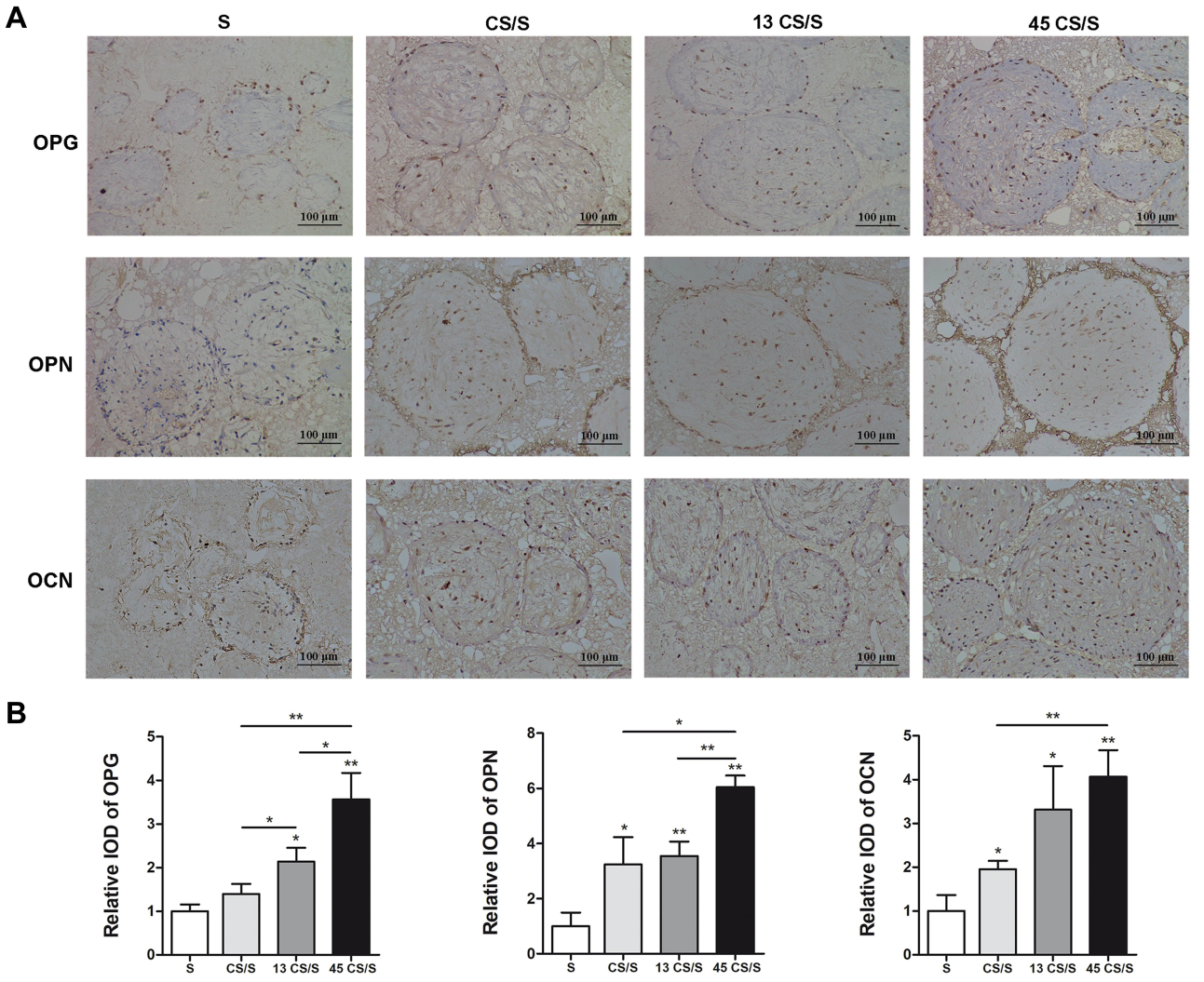

Figure 6 IHC staining of OPG, OPN, and OCN (**A**) and quantification (**B**) at 8 weeks. *p<0.05, **p<0.01.

osteogenic differentiation. COL1 is the most abundant protein in the ECM and acts as a scaffold for anchoring and distributing cells.[37] OPN is a major regulator of ECM mineralization and bone formation.[37] COL1 and OPN, these two ECM proteins fulfill the bone formation.

Previously, AuNPs have been reported to facilitate the osteogenic differentiation of mesenchymal stem cells through the p38/MAPK, ERK/MAPK, or Wnt/β-catenin signaling pathway.[18–21] However, mechanical stimulation by nanoparticles was recently found to cause biochemical changes and regulate signaling pathways, including all of the pathways mentioned above.[38] TEM observation showed that AuNPs were internalized through the endocytic pathway and trapped in lysosomes or autophagosomes.[39] In a recent study, it was demonstrated that cell mechanics dictated by cytoskeletal tension profoundly impact autophagic flux and cell phenotypic plasticity.[40] In this study, AuNP pretreatment resulted in activation of PDLSC autophagy with higher LC3II and lower p62 levels (Figure 4A). A few studies have also implied that autophagy has essential roles in the regulation of the differentiation and function of stem cells, osteoblasts, and osteocytes.[41] AuNPs might affect cytoskeletal structures through endocytosis and then promote osteogenic differentiation through autophagy activation. Similar results were obtained in other studies, where sliver, silica and hydroxyapatite nanoparticles were found to promote osteogenic differentiation of stem cells through activation of autophagy.[34,42,43] Data from existing studies have shown that the cellular uptake of AuNPs increases with increases in particle diameter between 10 and 50 nm.[44] Because 45-nm AuNPs were internalized more than 13-nm AuNPs, they induced

stronger biological effects.[45] Specifically, the 45-nm CS groups exhibited more autophagosomes and higher autophagic levels than the 13-nm CS groups in accord with a better differentiation potency before transplantation.[45,46]

The efficacy of AuNPs in promoting bone formation in PDLSC sheets was further observed in vivo. To avoid interference from the autologous stem cells of local bone tissue, a model of ectopic transplantation in immunodeficient mice was used. BCP scaffolds were selected because of their similar composition to bone matrix, bioactivity, and osteoconductivity.[47] The effectiveness of cell-based therapy depends on the retention and viability of cells after implantation. Cells labeled by GFP were used for tracking implanted cell sheets by histological examination. The green fluorescence was still observed after 4 weeks (Fig. S2). AuNPs were also found inside the cells in the BCP scaffold after 8 weeks, as indicated by HE staining (Fig. S3). These results implied that the implanted cells could survive and proliferate in vivo.

As a result, more new bone tissue formed inside the constructs in the AuNP groups in terms of micro-CT. AuNPs were also proven to distinctly improve the bone formation capacities of PDLSC sheets, as shown by bone-specific staining. AuNP treatment of PDLSC sheet/BCP constructs induced a significant increase in both osteoid and mineralized tissue. These PDLSCs from the cell sheets migrated inside the BCP scaffold, proliferated, differentiated into osteoblasts, mineralized, and thus induced bone formation.[48] The groups treated with 45-nm AuNPs showed more bone islands and greater mineralization than the groups treated with 13-nm AuNPs (Figure 5). In addition, 45-nm AuNPs promoted greater expression of bone-specific matrix proteins (OPG, OPN, and OCN) (Figure 6), which were highly expressed by osteoblasts and osteocytes.[37] All these results indicated that AuNPs, especially 45-nm AuNPs, could enhance osteogenic differentiation and matrix mineralization. However, it cannot be denied that there are differences between ectopic and orthotopic models, and further well-designed experiments in alveolar bone-defect models are needed to verify the osteogenic effects of AuNPs on PDLSC sheets.

Conclusion

AuNPs could enhance the osteogenesis of PDLSC sheets by activating autophagy, and 45-nm AuNPs was more effective than 13-nm AuNPs. This study determined the role of AuNPs in regulating the osteogenic differentiation and bone regeneration of PDLSC sheets, providing a new strategy for promoting the repair of alveolar bone defects.

Abbreviations

CST, Cell sheet technology; AuNPs, gold nanoparticles; PDLSC, periodontal ligament stem cell; ECM, extracellular matrix; TEM, transmission electron microscopy; ALP, Alkaline phosphatase; ARS, Alizarin red S staining; DAPI, 4′-6-diamidino-2-phenylindole; BCP, biphasic tricalcium phosphate; GFP, green fluorescent protein; IHC, immunohistochemistry.

Ethics Statement

This study received ethics approval from the Ethics Committee of Nanjing Stomatological Hospital, Medical School of Nanjing University, Nanjing, China (approval No. 2016NL-010(KS)). The written informed consent was obtained from each participant before the study. The study was carried out in accordance with the Declaration of Helsinki. All of the animal experimental procedures were approved by the Animal Ethics Committee of Nanjing University. The animal experimental were conducted according to policies and guidelines of the Institutional Animal Care and Use Committee of Nanjing University, Nanjing, China (No. SYXK 2019-0056).

Acknowledgments

This study was supported by the Natural Science Foundation of Jiangsu Province (No. BK20190133), the Fundamental Research Funds for the Central Universities (No. YK2005002) and the National Natural Science Foundation of China (No. 81570982).

Disclosure

The authors report no conflicts of interest in this work.

References

1. Pan J, Deng J, Yu L, et al. Investigating the repair of alveolar bone defects by gelatin methacrylate hydrogels-encapsulated human periodontal ligament stem cells. *J Mater Sci Mater Med*. 2019;31(1):3. doi:10.1007/s10856-019-6333-8
2. Chen FM, Sun HH, Lu H, Yu Q. Stem cell-delivery therapeutics for periodontal tissue regeneration. *Biomaterials*. 2012;33(27):6320–6344. doi:10.1016/j.biomaterials.2012.05.048
3. Novello S, Debouche A, Philippe M, Naudet F, Jeanne S. Clinical application of mesenchymal stem cells in periodontal regeneration: A systematic review and meta-analysis. *J Periodontal Res*. 2020;55(1):1–12. doi:10.1111/jre.12684
4. Bartold M, Gronthos S, Haynes D, Ivanovski S. Mesenchymal stem cells and biologic factors leading to bone formation. *J Clin Periodontol*. 2019;46(Suppl 21):12–32.

5. Chen M, Xu Y, Zhang T, et al. Mesenchymal stem cell sheets: a new cell-based strategy for bone repair and regeneration. *Biotechnol Lett*. 2019;41(3):305–318. doi:10.1007/s10529-019-02649-7
6. Kobayashi J, Kikuchi A, Aoyagi T, Okano T. Cell sheet tissue engineering: cell sheet preparation, harvesting/ manipulation, and transplantation. *J Biomed Mater Res A*. 2019;107(5):955–967. doi:10.1002/jbm.a.36627
7. Sekine H, Shimizu T, Dobashi I, et al. Cardiac cell sheet transplantation improves damaged heart function via superior cell survival in comparison with dissociated cell injection. *Tissue Eng Part A*. 2011;17(23–24):2973–2980. doi:10.1089/ten.tea.2010.0659
8. Seo BM, Miura M, Gronthos S, et al. Investigation of multipotent postnatal stem cells from human periodontal ligament. *Lancet*. 2004;364(9429):149–155. doi:10.1016/S0140-6736(04)16627-0
9. Feng F, Akiyama K, Liu Y, et al. Utility of PDL progenitors for in vivo tissue regeneration: a report of 3 cases. *Oral Dis*. 2010;16 (1):20–28. doi:10.1111/j.1601-0825.2009.01593.x
10. Chen FM, Gao LN, Tian BM, et al. Treatment of periodontal intrabony defects using autologous periodontal ligament stem cells: a randomized clinical trial. *Stem Cell Res Ther*. 2016;7:33. doi:10.1186/s13287-016-0288-1
11. Iwata T, Yamato M, Washio K, et al. Periodontal regeneration with autologous periodontal ligament-derived cell sheets–a safety and efficacy study in ten patients. *Regen Ther*. 2018;9:38–44. doi:10.1016/j.reth.2018.07.002
12. Xu Q, Li B, Yuan L, et al. Combination of platelet-rich plasma within periodontal ligament stem cell sheets enhances cell differentiation and matrix production. *J Tissue Eng Regen Med*. 2017;11 (3):627–636. doi:10.1002/term.1953
13. Lin J, Shao J, Juan L, et al. Enhancing bone regeneration by combining mesenchymal stem cell sheets with β-TCP/COL-I scaffolds. *J Biomed Mater Res B Appl Biomater*. 2018;106(5):2037–2045. doi:10.1002/jbm.b.34003
14. Yan J, Zhang C, Zhao Y, et al. Non-viral oligonucleotide antimiR-138 delivery to mesenchymal stem cell sheets and the effect on osteogenesis. *Biomaterials*. 2014;35(27):7734–7749. doi:10.1016/j.biomaterials.2014.05.089
15. Wang Q, Yan J, Yang J, Li B. Nanomaterials promise better bone repair. *Mater Today*. 2016;19(8):451–463. doi:10.1016/j.mattod.2015.12.003
16. Bodelon G, Costas C, Perez-Juste J, Pastoriza-Santos I, Liz-Marzan LM. Gold nanoparticles for regulation of cell function and behavior. *Nano Today*. 2017;13:40–60. doi:10.1016/j.nantod.2016.12.014
17. Vial S, Reis RL, Miguel Oliveira J. Recent advances using gold nanoparticles as a promising multimodal tool for tissue engineering and regenerative medicine. *Curr Opin Solid St M*. 2017;21 (2):92–112. doi:10.1016/j.cossms.2016.03.006
18. Yi C, Liu D, Fong -C-C, Zhang J, Yang M. Gold nanoparticles promote osteogenic differentiation of mesenchymal stem cells through p38 MAPK pathway. *ACS Nano*. 2010;4(11):6439–6448. doi:10.1021/nn101373r
19. Zhang D, Liu D, Zhang J, Fong C, Yang M. Gold nanoparticles stimulate differentiation and mineralization of primary osteoblasts through the ERK/MAPK signaling pathway. *Mater Sci Eng C Mater Biol Appl*. 2014;42:70–77. doi:10.1016/j.msec.2014.04.042
20. Choi SY, Song MS, Ryu PD, Lam ATN, Joo S-W, Lee SY. Gold nanoparticles promote osteogenic differentiation in human adipose-derived mesenchymal stem cells through the Wnt/β-catenin signaling pathway. *Int J Nanomedicine*. 2015;10:4383–4392. doi:10.2147/IJN.S78775
21. Liang H, Xu X, Feng X, et al. Gold nanoparticles-loaded hydroxyapatite composites guide osteogenic differentiation of human mesenchymal stem cells through Wnt/β-catenin signaling pathway. *Int J Nanomedicine*. 2019;14:6151–6163. doi:10.2147/IJN.S213889
22. Lee D, Heo DN, Kim H-J, et al. Inhibition of osteoclast differentiation and bone resorption by bisphosphonate-conjugated gold nanoparticles. *Sci Rep*. 2016;6:27336. doi:10.1038/srep27336
23. Heo DN, Ko W-K, Bae MS, et al. Enhanced bone regeneration with a gold nanoparticle–hydrogel complex. *J Mater Chem B*. 2014;2 (11):1584–1593. doi:10.1039/C3TB21246G
24. Zhang Y, Wang P, Mao H, et al. PEGylated gold nanoparticles promote Osteogenic differentiation in in vitro and in vivo systems. *Mater Design*. 2020;109231.
25. Zhang Y, Kong N, Zhang Y, Yang W, Yan F. Size-dependent effects of gold nanoparticles on osteogenic differentiation of human periodontal ligament progenitor cells. *Theranostics*. 2017;7(5):1214–1224. doi:10.7150/thno.17252
26. Iwata T, Washio K, Yoshida T, et al. Cell sheet engineering and its application for periodontal regeneration. *J Tissue Eng Regen Med*. 2015;9(4):343–356. doi:10.1002/term.1785
27. Kim H, Kim Y, Park J, Hwang NS, Lee YK, Hwang Y. Recent advances in engineered stem cell-derived cell sheets for tissue regeneration. *Polymers*. 2019;11(2):209. doi:10.3390/polym11020209
28. Vorotnikova E, McIntosh D, Dewilde A, et al. Extracellular matrix-derived products modulate endothelial and progenitor cell migration and proliferation in vitro and stimulate regenerative healing in vivo. *Matrix Biol*. 2010;29(8):690–700. doi:10.1016/j.matbio.2010.08.007
29. Pei M, Li J, Shoukry M, Zhang Y. A review of decellularized stem cell matrix: a novel cell expansion system for cartilage tissue engineering. *Eur Cell Mater*. 2011;22:333–343. doi:10.22203/eCM.v022a25
30. Wei F, Qu C, Song T, et al. Vitamin C treatment promotes mesenchymal stem cell sheet formation and tissue regeneration by elevating telomerase activity. *J Cell Physiol*. 2012;227(9):3216–3224. doi:10.1002/jcp.24012
31. Qi Y, Wang Y, Yan W, Li H, Shi Z, Pan Z. Combined mesenchymal stem cell sheets and rhBMP-2-releasing calcium sulfate-rhBMP-2 scaffolds for segmental bone tissue engineering. *Cell Transplant*. 2012;21(4):693–705. doi:10.3727/096368911X623844
32. Chen G, Fang T, Qi Y, et al. Combined use of mesenchymal stromal cell sheet transplantation and local injection of SDF-1 for bone repair in a rat nonunion model. *Cell Transplant*. 2016;25(10):1801–1817. doi:10.3727/096368916X690980
33. Wang Q, Chen B, Cao M, et al. Response of MAPK pathway to iron oxide nanoparticles in vitro treatment promotes osteogenic differentiation of hBMSCs. *Biomaterials*. 2016;86:11–20. doi:10.1016/j.biomaterials.2016.02.004
34. He W, Zheng Y, Feng Q, et al. Silver nanoparticles stimulate osteogenesis of human mesenchymal stem cells through activation of autophagy. *Nanomedicine*. 2020;15(4):337–353. doi:10.2217/nnm-2019-0026
35. Gersbach CA, Byers BA, Pavlath GK, García AJ. Runx2/Cbfa1 stimulates transdifferentiation of primary skeletal myoblasts into a mineralizing osteoblastic phenotype. *Exp Cell Res*. 2004;300 (2):406–417. doi:10.1016/j.yexcr.2004.07.031
36. Komori T. Regulation of osteoblast differentiation by transcription factors. *J Cell Biochem*. 2006;99(5):1233–1239. doi:10.1002/jcb.20958
37. Lin X, Patil S, Gao YG, Qian A. The bone extracellular matrix in bone formation and regeneration. *Front Pharmacol*. 2020;11:757. doi:10.3389/fphar.2020.00757
38. Septiadi D, Crippa F, Moore TL, Rothen-Rutishauser B, Petri-Fink A. Nanoparticle-cell interaction: a cell mechanics perspective. *Adv Mater*. 2018;30(19):e1704463. doi:10.1002/adma.201704463
39. Liu Y, Zhou H, Yin T, et al. Quercetin-modified gold-palladium nanoparticles as a potential autophagy inducer for the treatment of Alzheimer's disease. *J Colloid Interface Sci*. 2019;552:388–400. doi:10.1016/j.jcis.2019.05.066
40. Totaro A, Zhuang Q, Panciera T, et al. Cell phenotypic plasticity requires autophagic flux driven by YAP/TAZ mechanotransduction. *Proc Natl Acad Sci U S A*. 2019;116(36):17848–17857. doi:10.1073/pnas.1908228116

41. Jaber FA, Khan NM, Ansari MY, Al-Adlaan AA, Hussein NJ, Safadi FF. Autophagy plays an essential role in bone homeostasis. *J Cell Physiol*. 2019;234(8):12105–12115. doi:10.1002/jcp.27071
42. Ha S-W, Weitzmann MN, Beck JGR. Bioactive silica nanoparticles promote osteoblast differentiation through stimulation of autophagy and direct association with LC3 and p62. *ACS Nano*. 2014;8 (6):5898–5910. doi:10.1021/nn5009879
43. Wang R, Hu H, Guo J, et al. Nano-hydroxyapatite modulates osteoblast differentiation through autophagy induction via mTOR signaling pathway. *J Biomed Nanotechnol*. 2019;15(2):405–415. doi:10.1166/jbn.2019.2677
44. Jiang W, Kim BY, Rutka JT, Chan WC. Nanoparticle-mediated cellular response is size-dependent. *Nat Nanotechnol*. 2008;3 (3):145–150. doi:10.1038/nnano.2008.30
45. Ma X, Wu Y, Jin S, et al. Gold nanoparticles induce autophagosome accumulation through size-dependent nanoparticle uptake and lysosome impairment. *ACS Nano*. 2011;5(11):8629–8639. doi:10.1021/nn202155y
46. Chithrani BD, Chan WC. Elucidating the mechanism of cellular uptake and removal of protein-coated gold nanoparticles of different sizes and shapes. *Nano Lett*. 2007;7(6):1542–1550. doi:10.1021/nl070363y
47. Jeong J, Kim JH, Shim JH, Hwang NS, Heo CY. Bioactive calcium phosphate materials and applications in bone regeneration. *Biomater Res*. 2019;23:4. doi:10.1186/s40824-018-0149-3
48. Kira T, Akahane M, Omokawa S, et al. Bone regeneration with osteogenic matrix cell sheet and tricalcium phosphate: an experimental study in sheep. *World J Orthop*. 2017;8(10):754–760. doi:10.5312/wjo.v8.i10.754